SIX-SIDED HEPTAPORPHYRIN ARRAY: TOWARDS A NANO-SIZED CUBE

Steven J. LANGFORD[1,*] and Clint P. WOODWARD[2]

School of Chemistry, Monash University, Clayton, Victoria 3800, Australia;
e-mail: [1] steven.langford@sci.monash.edu.au; [2] clint.woodward@sci.monash.edu.au

Received December 16, 2003
Accepted March 12, 2004

Dedicated to Professor Ivan Stibor on the occasion of his 60th birthday in recognition of his outstanding contributions to supramolecular chemistry.

A strategy in preparing a family of hexameric porphyrin cubes based on the interplay of Sn(IV)–O and Ru(II)–N interactions is described. In this first iteration, we have prepared the heptamer $[Sn^{IV}(TPyP)\cdot(\mathbf{4})_2][Ru(CO)(TPP)]_6$ (**4** = (*E*)-(3-(4-pyridyl)acrylate)) constituting a 5,10,15,20-tetra(4-pyridyl)porphyrin (TPyP) core and 5,10,15,20-tetraphenylporphyrin (TPP) faces and compared its formation by stepwise and "one-pot" strategies where up to nine components are assembled in a single step in a regiospecific manner. In one example, the heptamer is formed around the template $[Sn^{IV}(TPyP)\cdot(\mathbf{4})_2]$ bearing pyridine groups in which the nitrogens radiate octahedrally along each vertex. The ability to modulate the axial vertex through choice of pyridine is also demonstrated. ^{1}H NMR measurements on $[Sn^{IV}(TPyP)\cdot(\mathbf{4})_2][Ru(CO)(TPP)]_6$ indicate that the protons on the core template are extremely shielded as a result of the anisotropy of the peripheral porphyrin units. Various NMR techniques, including NOESY experiments, have been used to characterise the heptamer in solution.

Keywords: Porphyrinoids; Porphyrins; Coordination; Ruthenium; Tin(IV); Supramolecular chemistry; Self-assembly; Tectons; Coordination dendrimers.

Multiporphyrin systems in which the porphyrin subunits are interlinked using traditional covalent bonds[1–3] or via self-assembly processes[4] involving metal coordination[5–12] have produced an array of elegant structures designed to address aspects of photosynthetic mimicry, host–guest complexation or catalysis. From our point of view, the D_{4h} symmetry of the porphyrin macrocycle combined with its planar nature should allow the generation of a range of nano-sized molecular cubes that may be restrictive (based on the linking of porphyrinic *meso* groups on adjacent faces in a covalent fashion) or non-restrictive in which the orientation of each face is free to rotate with respect to its neighbouring faces. Our motivation for the

doi:10.1135/cccc20040996

design and synthesis of molecules with a cube-like geometry[13] is drawn from the parallels such geometries have in the macroscopic world with respect to both the internal (box-like) cavity (Fig. 1a) and external (block-like) surface (Fig. 1b). Provided the correct steric and electronic features are present, molecular cubes incorporating photoactive elements[14] (e.g., free-base or Zn(II) porphyrins) could be used as building blocks for the construction of three-dimensional assemblies, with potential use as light-harvesting systems (Fig. 1b). The internal cavity of a cube (Fig. 1a) may also serve as a receptor to small molecules or act as a carcerand[15] by trapping larger molecules unable to leave the confines of the "cage" structure[16]. In such situations, metalloporphyrin derivatives may show catalytic activity, especially if a mixed-metal species can be generated suprafacially.

The strategy we have undertaken in generating both restrictive and non-restrictive porphyrin-based cubes builds on the previous work of Alessio[6], Hupp[7], Stang[8], Lehn[9], Sanders[10] and from our laboratory[11] (Fig. 2). Within this historical context, combining *pseudo* two-dimensional porphyrin pentamers[6] and tetramers[7–9] (Fig. 2a, 2b) with *pseudo* one-dimensional porphyrin trimers[10,11] (Fig. 2c) should generate a three-dimensional structure in which the six faces of the resultant cube are porphyrinic (Fig. 2d). The formation of an octahedral template derived from tetra(4-pyridyl)porphyrin (Fig. 2e) is central to our approach. The radiating pyridines are able to complex to a range of Zn(II) and Ru(II) porphyrins generating a cube-like architecture which, provided the correct functionality can be introduced to the *meso* position, should also allow for their eventual covalent attachment into a restrictive cube. Here we describe the formation of the *pseudo*-octahedral components **1**–**4** (Scheme 1) which dif-

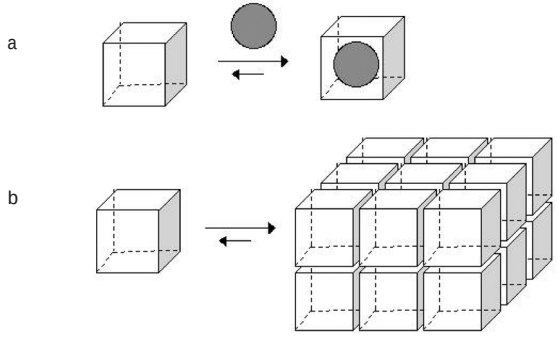

FIG. 1
a A cube-shaped receptor acting as a convergent receptor; b the same receptor acting in a divergent fashion may self-assemble in a building block fashion

fer in their elongation about the axial components, the evolution of $[Sn^{IV}(TPyP)\cdot(\mathbf{4})_2]$ (TPyP = 5,10,15,20-tetra(4-pyridyl)-21*H*,23*H*-porphyrin, **4** = (*E*)-3-(4-pyridyl)acrylaic acid) into a non-restrictive cube, and evaluate the efficiency of a one-pot process involving the self-assembly of six porphyrins about the centre of **4** against a stepwise convergent approach.

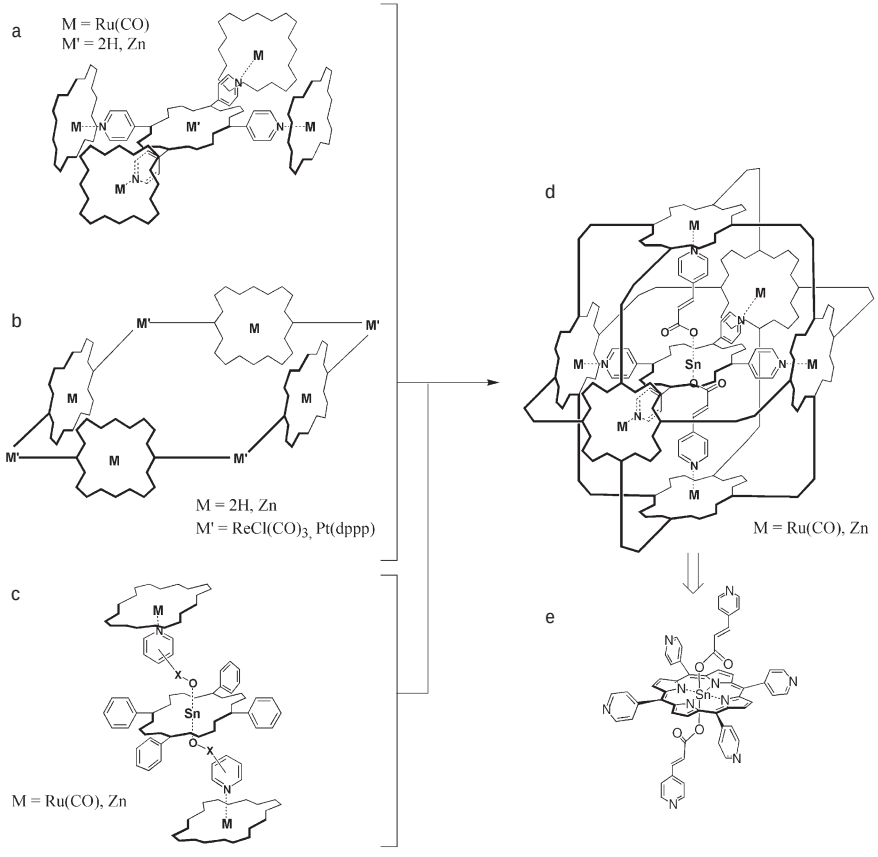

FIG. 2

The development of a molecular cube using porphyrins as the faces is plausible: a Alesio's early work on assembling porphyrins around a tetrapyridyl centre; b the independent work of Lehn, Hupp and Stang have formed porphyrin squares using different metal ions at the vertices; c cofacial mixed porphyrin stacks using carboxylic acids and phenols have been prepared. The union of a–c leads to d a covalently bound (restrictive) porphyrinic cube into which a suitable octahedral component e has been inserted. Peripheral groups have been removed for clarity

EXPERIMENTAL

General Comments

Chemicals were purchased from Aldrich and Lancaster and used as received. Melting points were measured on a Stuart Scientific melting point apparatus. Low-resolution mass spectra were recorded on a Micromass Platform II spectrometer. Samples were ionised using an electrospray ionisation (ESI) source and recorded as the solutions specified. ^{1}H and ^{13}C NMR spectra (δ, ppm; *J*, Hz) were recorded using a Bruker DPX 300 MHz spectrometer (300 MHz ^{1}H, 75 MHz ^{13}C) or a Bruker DRX 400 MHz spectrometer (400 MHz ^{1}H, 100 MHz ^{13}C) as solutions in the deuterated solvents specified. Chemical shifts (δ) were calibrated against the residual solvent peak. ^{13}C NMR spectra were recorded using the JMOD pulse sequence or proton decoupled pulse sequence. NOESY and HSQC experiments were carried out on a Bruker DRX500 NMR spectrometer operating at 500 MHz using standard pulse sequences. UV-VIS spectra (in nm) were recorded on a Varian model Cary 100 Bio spectrophotometer in the solvent specified.

Syntheses

[Sn^{IV}(OH)$_2$(TPyP)]. A solution of TPyP (500 mg, 0.81 mmol) and $SnCl_2$ (766 mg, 4.04 mmol) in pyridine (80 ml) was mixed at reflux for 24 h in the dark. Upon completion, the reaction mixture was quenched with aqueous ammonia solution (25% (v/v), 100 ml) and was left to stir for 30 min. The mixture was poured into water (250 ml) and then extracted with dichloromethane (3 × 75 ml). The combined extracts were dried over anhydrous Na_2SO_4, filtered and solvent removed in vacuo. The residue was recrystallised from chloroform/methanol to yield [Sn^{IV}(OH)$_2$(TPyP)] (470 mg, 76%) as a fine pink-purple powder. M.p. > 350 °C. ^{1}H NMR (300 MHz, $CDCl_3$): 8.29 d, 8 H, *J* = 5.9 (*m*-Py); 9.14 d, 8 H, *J* = 5.9 (*o*-Py); 9.18 s, 8 H (β-pyrrolic H). ^{13}C NMR (75 MHz, $CDCl_3$): 119.0, 129.7, 133.2, 146.2, 148.9, 149.0. MS (ESI, +ve), *m/z*: 771.5 [M + H]$^{+}$.

[Sn^{IV}(OH)$_2$(TPyP)][Ru(CO)(TPP)]$_4$. Synthesis of the title compound followed a procedure similar to that of Alessio et al.[6] A solution of [Sn^{IV}(OH)$_2$(TPyP)] (100 mg, 0.13 mmol) and carbonyl(5,10,15,20-tetraphenyl-21*H*,23*H*-porphinato)ruthenium(II), [Ru(CO)(TPP)]·EtOH (where TPP = 5,10,15,20-tetraphenyl-21*H*,23*H*-porphyrin), (409.6 mg, 0.52 mmol) in chloroform (100 ml) was stirred at room temperature for 2 days in the dark. Upon completion, the solvent volume was reduced to 10 ml and diethyl ether (50 ml) was added to the red solution. The resulting precipitate was filtered off and washed with diethyl ether to give [Sn^{IV}(OH)$_2$(TPyP)][Ru(CO)(TPP)]$_4$ (383 mg, 79%) as a fine dark red powder. M.p. > 350 °C. UV-VIS ($CHCl_3$), λ_{max} (log ε): 411 (6.09), 423 (5.89) sh, 530 (4.97), 560 (4.58), 596 (4.02). ^{1}H NMR (300 MHz, $CDCl_3$): 1.80 d, 8 H, *J* = 6.5 (*o*-PyH); 5.63 d, 8 H, *J* = 6.5 (*m*-PyH); 7.00 s, 8 H (β-pyrrolic H on Sn(TPyP)); 7.55 t, 16 H, *J* = 7.4 (*meso*-ArH on Ru(TPP)); 7.75 p, 32 H, *J* = 7.7 (*meso*-ArH on Ru); 7.99 d, 16 H, *J* = 7.4 (*meso*-ArH on Ru(TPP)); 8.29 d, 16 H, *J* = 7.4 (*meso*-ArH on Ru(TPP)); 8.68 s, 32 H (β-pyrrolic H on Ru(TPP)). ^{13}C NMR (75 MHz, $CDCl_3$): 122.0, 126.5, 126.9, 127.0, 127.7, 132.2, 134.1, 134.7, 142.7, 143.0, 144.7.

*[Ru(CO)(TPP)·(**4**)]*. A solution of [Ru(CO)(TPP)]·EtOH (100 mg, 0.127 mmol), (*E*)-3-(4-pyridyl)acrylic acid (**4**) (18.9 mg, 0.127 mmol) and potassium carbonate (17.4 mg, 0.127 mmol) in chloroform (25 ml) was stirred at reflux for 2 days in the dark. Upon completion, the chloroform was removed in vacuo to give [Ru(CO)(TPP)·(**4**)] (109 mg, 96%) as shiny dark purple crystals. ^{1}H NMR (300 MHz, $CDCl_3$): 1.29 d, 2 H, *J* = 6.3 (*o*-PyH); 4.66 d,

2 H, *J* = 6.3 (*m*-PyH); 4.79 d, 1 H, *J* = 15.7 (C=C-H); 5.31 d, 1 H, *J* = 15.7 (C=C-H); 7.39 t, 4 H, *J* = 6.8 (*meso*-ArH); 7.63 t, 4 H, *J* = 7.2 (*meso*-ArH); 7.75 t, 4 H, *J* = 7.5 (*meso*-ArH); 7.82 d, 4 H, *J* = 7.5 (*meso*-ArH); 8.20 d, 4 H, *J* = 7.7 (*meso*-ArH); 8.47 s, 8 H (β-pyrrolic H). ^{13}C NMR (75 MHz, $CDCl_3$): 119.2, 121.8, 126.3, 127.0, 127.6, 132.0, 134.0, 134.7, 142.7, 143.7, 144.3, 171.1.

Syntheses of Octahedral Tectons

*[Sn^{IV}(TPyP)·(**1**)$_2$]*. A solution of [Sn^{IV}(OH)$_2$(TPyP)] (25.6 mg, 0.032 mmol) and 3-hydroxypyridine (**1**) (6.2 mg, 0.065 mmol) in chloroform (10 ml) was stirred at room temperature for 24 h in the dark. Upon completion, the solvent removed and the product recrystallised from chloroform/methanol to give [Sn^{IV}(TPyP)·(**1**)$_2$] as a fine purple powder (25.6 mg, 85%). M.p. > 350 °C. ^{1}H NMR (300 MHz, $CDCl_3$): 2.18 dq, 2 H, *J* = 8.2, 1.5 (ax PyH); 3.14 d, 2 H, *J* = 2.8 (ax PyH); 5.62 dd, 2 H, *J* = 8.2, 4.5 (ax PyH); 7.06 d, 2 H, *J* = 3.5 (ax PyH); 8.15 d, 8 H, *J* = 5.9 (eq *m*-PyH); 9.15 d, 8 H, *J* = 5.9 (eq *o*-PyH); 9.18 s, 8 H (β-pyrrolic H on Sn(TPyP)). ^{13}C NMR (75 MHz, $CDCl_3$): 119.9, 121.4, 122.8, 123.9, 129.5, 133.4, 138.4, 140.1, 146.9, 148.1, 149.1. MS (ESI, +ve), *m/z*: 927 $[M + H]^+$.

General Method for Ligand Exchange – Preparation of [Sn^{IV}(TPyP)·(**2**–**4**)$_2$]

To a solution of [Sn^{IV}(OH)$_2$(TPyP)] (25 mg, 0.03 mmol) and carboxylic acid **2**–**4** (Scheme 1) (2.2 equivalents) in chloroform (10 ml), K_2CO_3 (2.2 equivalents) was added and the mixture was stirred at reflux for 24 h in the dark. Upon completion, the reaction mixture was filtered and the solvent removed to give [Sn^{IV}(TPyP)·(**2**–**4**)$_2$] as a fine purple powder. The product was recrystallised from chloroform/methanol.

*[Sn^{IV}(TPyP)·(**2**)$_2$]*. Yield 68%. M.p. > 350 °C. ^{1}H NMR (300 MHz, $CDCl_3$): 4.80 d, 4 H, *J* = 5.9 (ax *m*-PyH); 7.64 d, 4 H, *J* = 5.9 (ax *o*-PyH); 8.22 d, 8 H, *J* = 5.9 (eq *m*-PyH); 9.14 d, 8 H, *J* = 5.9 (eq *o*-PyH); 9.26 s, 8 H (β-pyrrolic H). ^{13}C NMR (75 MHz, $CDCl_3$): 117.9, 119.6, 128.1, 128.6, 132.0, 145.1, 145.4, 147.5, 147.7.

*[Sn^{IV}(TPyP)·(**3**)$_2$]*. Yield 78%. M.p. > 350 °C. ^{1}H NMR (300 MHz, $CDCl_3$): 0.65 s, 4 H (CH_2); 5.07 dt, 2 H, *J* = 7.7, 1.8 (ax PyH); 6.04 d, 2 H, *J* = 2.3 (ax PyH); 6.40 dd, 2 H, *J* = 7.7, 4.8 (ax PyH); 8.00 dd, 2 H, *J* = 4.9, 1.7 (ax PyH); 8.20 d, 8 H, *J* = 5.9 (eq *m*-PyH); 9.13 d, 8 H, *J* = 5.9 (eq *o*-PyH); 9.16 s, 8 H (β-pyrrolic H). ^{13}C NMR (75 MHz, $CDCl_3$): 37.6, 118.0, 120.7, 128.2, 129.0, 131.8, 132.9, 131.8, 145.2, 147.7, 147.5, 147.2, 165.2. MS (ESI, +ve), *m/z*: 1031 $[M + H]^+$.

*[Sn^{IV}(TPyP)·(**4**)$_2$]*. Yield 79%. M.p. > 350 °C. UV-VIS ($CHCl_3$), λ_{max} (log ε): 400 (4.42), 423 (5.53), 556 (4.15), 594 (3.54). ^{1}H NMR (300 MHz, $CDCl_3$): 3.70 d, 2 H, *J* = 15.9 (alkene H); 4.30 d, 2 H, *J* = 15.9 (alkene H); 6.23 d, 4 H, *J* = 6.2 (ax *m*-PyH); 8.13 d, 4 H, *J* = 6.2 (ax *o*-PyH); 8.26 d, 8 H, *J* = 5.9 (eq *m*-PyH); 9.13 d, 8 H, *J* = 5.9 (eq *o*-PyH); 9.28 s, 8 H (β-pyrrolic H). ^{13}C NMR (75 MHz, $CDCl_3$): 119.6, 120.9, 125.2, 129.5, 133.2, 136.2, 141.6, 146.9, 148.6, 149.0, 150.0.

Porphyrin Heptamer [Sn^{IV}(TPyP)·(**4**)$_2$][Ru(CO)(TPP)]$_6$

Method A. A solution of [Sn^{IV}(OH)$_2$(TPyP)][Ru(CO)(TPP)]$_4$ (5.0 mg, 1.3 μmol) and [Ru(CO)(TPP)·(**4**)] (2.4 mg, 2.6 μmol) in $CHCl_3$ (3 ml) was stirred at reflux in a sealed tube for 7 days in the dark. After completion, the solvent was removed and the residue chromatographed (neutral alumina, $CHCl_3$) to yield the heptamer (3.4 mg, 48%) as a red-purple

powder. M.p. > 350 °C. UV-VIS ($CHCl_3$), λ_{max} (log ε): 409 (6.17), 527 (4.95), 553 (4.08) sh, 594 (4.00). ^{1}H NMR (300 MHz, $CDCl_3$): 0.70 d, 4 H, *J* = 6.8 (ax *o*-PyH); 1.25 d, 2 H, *J* = 15.9 (alkene H); 1.61 d, 8 H, *J* = 6.5 (eq *o*-PyH); 2.60 d, 2 H, *J* = 15.9 (alkene H); 3.44 d, 4 H, *J* = 6.8 (ax *m*-PyH); 5.33 d, 8 H, *J* = 6.5 (eq *m*-PyH); 6.77 s, 8 H (β-pyrrolic H on Sn(TPyP)); 7.44–7.61 m, 30 H (*meso*-ArH on Ru(TPP)); 7.70–7.91 m, 66 H (*meso*-ArH on Ru(TPP)); 7.87 m, 16 H (*meso*-ArH on Ru(TPP)); 8.08–8.12 m, 8 H (*meso*-ArH on Ru(TPP)); 8.26–8.29 m, 16 H (*meso*-ArH on Ru(TPP)); 8.40 s, 16 H (ax β-pyrrolic H on Ru(TPP)); 8.64 s, 32 H (eq β-pyrrolic H on Ru(TPP)).

Method B. A solution of [Sn^{IV}(TPyP)·(**4**)$_2$] (2.5 mg, 9.7 μmol) and [Ru(CO)(TPP)] (47.6 mg, 58.1 μmol) in $CHCl_3$ (3 ml) was stirred at reflux in a sealed tube for 2 days in the dark. After completion, the solvent was removed and the residue chromatographed (neutral alumina, $CHCl_3$) to yield the heptamer (25 mg, 47%) as a red-purple powder. This product was identical spectroscopically to that described in method *A*.

Method C, one-pot process. To a solution of Sn^{IV}(TPyP) (2.5 mg, 3.2 μmol), **4** (1.0 mg, 6.4 μmol) and [Ru(CO)(TPP)] (15.5 mg, 19.5 μmol) in $CHCl_3$ (3 ml), K_2CO_3 was added (0.9 mg, 6.4 μmol) and the resulting solution was stirred at reflux in a sealed tube for 2 days in the dark. After completion, the solvent was removed and the residue chromatographed (neutral alumina, $CHCl_3$) to yield the heptamer (11.6 mg, 66%) as a red-purple powder. This product was identical spectroscopically to that described in method *A*.

RESULTS AND DISCUSSION

Octahedral Tectons

The synthesis of a series of octahedral tectons that incorporate pyridine groups extended along each of the vertices is shown in Scheme 1. In this

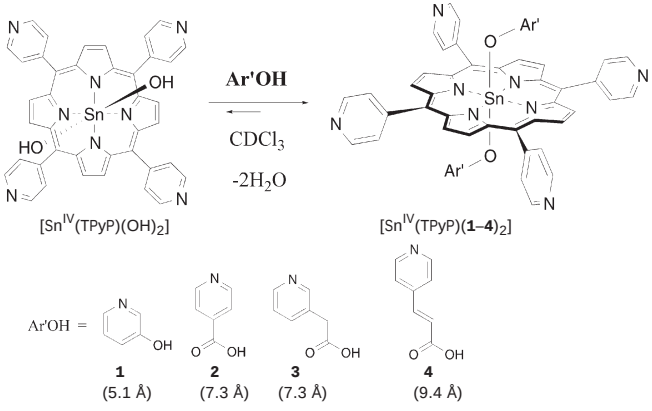

SCHEME 1

General synthesis of the octahedral tectons using **1**–**4**. The orthogonal distances between the pyridine nitrogen and the porphyrin plane for each Sn(IV) complex, as assigned by molecular modelling (*Accelrys*), are shown in the parentheses. Potassium carbonate is also added as a reagent for carboxylic acids **2**–**4**

series, we have used both phenol- and carboxylic acid-based moieties to modulate the distance between the axial pyridines and the porphyrin plane. The reaction takes advantage of both the oxophilic nature of Sn(IV) porphyrins[17,18] to specifically functionalise the porphyrin core and the D_{4h} geometry of the porphyrin macrocycle to induce the *pseudo*-octahedral geometry of the tecton.

Time-dependent ^{1}H NMR spectra of [$Sn^{IV}(OH)_2$(TPyP)], taken at 300 K in $CDCl_3$ after the addition of 2.0 equivalents of phenol (**1**) and initial mixing, give sharp signals corresponding to (i) [$Sn^{IV}(OH)_2$(TPyP)], (ii) pyridine, (iii) a set of resonances judged to be a 1:1 complex, and (iv) a significantly smaller proportion of the 1:2 complex. In all cases, the situation is one of slow kinetics at 300 MHz and 300 K. Over time (ca. 120 min) the proportion of each component in solution changes until the only species in solution can be attributed to water (from the ligand exchange reaction) and the octahedral tecton (Scheme 1). The situation for carboxylic acids **2**–**4** is different based on their zwitterionic nature, which leads to solubility problems in the solvent of choice. Reactions of [$Sn^{IV}(OH)_2$(TPyP)] with **2**–**4** were undertaken in the presence of potassium carbonate, which aids in the ligand exchange. In each case, the stoichiometry is readily determined as 1:2 by integration of relevant probe protons on both the Sn(IV) porphyrin and the axial pyridine. Changes ($\Delta\delta$) of selected resonances in the ^{1}H NMR spectra for [Sn^{IV}(TPyP)·(**1**)$_2$] and [Sn^{IV}(TPyP)·(**4**)$_2$][Ru(CO)(TPP)]$_6$ against **1** and [Ru(CO)(TPP)·(**4**)] are shown in Fig. 3. The very large chemical shift changes observed upon ligand exchange of phenol **1** or [Ru(CO)(TPP)·(**4**)] are a result of the time-averaged orientation and proximity of these nuclei

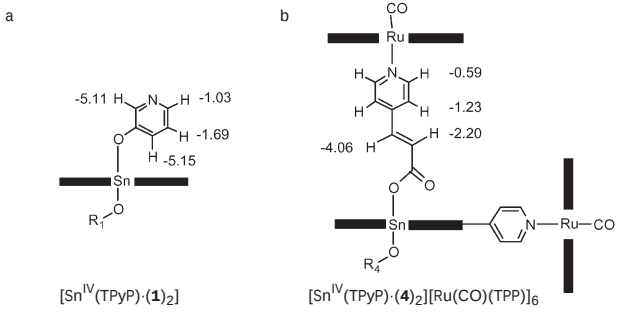

FIG. 3

Porphyrin-induced chemical shift changes (300 MHz) a for [Sn^{IV}(TPyP)·(**1**)$_2$] ($\Delta\delta$ = δ(complex) – δ(free phenol)) and b for the heptameric porphyrin cube ($\Delta\delta$ = δ(complex) – δ(**4**·[Ru(CO)(TPP)]). Due to the insolubility of the carboxylic acids **2**–**4** in $CDCl_3$ no comparison can be made between the free and complexed species

to the porphyrin ring current. Purely on this basis and as expected, the chemical shift differences ($\Delta\delta$) associated with the phenolic ligand are significantly larger than those associated with similar carboxylic acid species[17,19]. Despite significant effort, the complexes $[Sn^{IV}(TPyP)\cdot(\mathbf{2})_2]$ and $[Sn^{IV}(TPyP)\cdot(\mathbf{4})_2]$ failed to show a parent ion peak by either electrospray mass ionisation (ESI-MS), fast atom bombardment (FAB-MS) or matrix-assisted laser desorption (MALDI) mass spectrometry.

Stepwise Approach to $[Sn^{IV}(TPyP)\cdot(\mathbf{4})_2][Ru(CO)(TPP)]_6$

Based on the geometry of the cube and the dimensions of each peripheral component, we surmised that $[Sn^{IV}TTP\cdot(\mathbf{4})_2]$ might provide a useful template for a porphyrin cube, since its 11.6 Å Sn–Ru_{ax} distance[20,21] is most comparable to that needed to match the 9.4 Å distance between antipodal *meso p*-phenyl hydrogens. The formation of the heptameric porphyrin cube $[Sn^{IV}(TPyP)\cdot(\mathbf{4})_2][Ru(CO)(TPP)]_6$ was achieved via stepwise and one-pot strategies (Scheme 2).

We have been interested in using metalloporphyrin derivatives of Alessio's pentamer as a distant analogue to calixarenes for the complexation of large molecular entities[22] and chose it as the starting point of our synthetic scheme. Metallation of H_2TPyP ($SnCl_2$, pyridine, reflux) afforded $[Sn^{IV}(OH)_2(TPyP)]$ in 76% yield, which, when reacted with four equivalents of [Ru(CO)(TPP)] ($CHCl_3$, reflux, 2 days) yields $[Sn^{IV}(OH)_2(TPyP)][Ru(CO)(TPP)]_4$ in 79% yield (Scheme 2). The Sn(IV) pentamer $[Sn^{IV}(OH)_2(TPyP)][Ru(CO)(TPP)]_4$ has two axial hydroxy groups that are susceptible to ligand exchange with phenols or carboxylic acids to yield the corresponding phenolate or carboxylate complexes, respectively. Reaction of $[Sn^{IV}(OH)_2(TPyP)][Ru(CO)(TPP)]_4$ with $[Ru(CO)(TPP)\cdot(\mathbf{4})]$ ($CHCl_3$, reflux, 7 days) yielded the heptameric porphyrin cube $[Sn^{IV}(TPyP)\cdot(\mathbf{4})_2][Ru(CO)(TPP)]_6$ in 48% yield after chromatography on neutral alumina ($CHCl_3$). Integration of probe protons associated with the axial ligands, the Sn(IV) β-pyrrolic protons and two types of magnetically non-equivalent Ru porphyrins readily confirm the stoichiometry of $[Sn^{IV}(TPyP)]$:**4**:[Ru(CO)(TPP)] to be 1:2:6, consistent with the formation of the heptameric structure $[Sn^{IV}(TPyP)\cdot(\mathbf{4})_2][Ru(CO)(TPP)]_6$ (Scheme 2). Chemical shift differences between $[Ru(CO)(TPP)\cdot(\mathbf{4})]$ and $[Sn^{IV}(TPyP)\cdot(\mathbf{4})_2][Ru(CO)(TPP)]_6$ in $CDCl_3$ are shown schematically in Fig. 3 and provide evidence for the formation of the heptameric cube. The sum of the peripheral porphyrin ring currents experienced by the protons on **4** lead to the large chemical shift changes in the ^1H NMR spectrum. The process is slow and stepwise, as evidenced by the appearance

and disappearance of signals at δ 7.00 and 6.88, attributable to the β-pyrrolic protons of the Sn(IV) porphyrin in $[Sn^{IV}(OH)_2(TPyP)][Ru(CO)(TPP)]_4$ and $[Sn^{IV}(OH)(TPyP)\cdot(\mathbf{4})][Ru(CO)(TPP)]_5$, respectively, culminating in a set of resonances at δ 6.77 attributable to the product $[Sn^{IV}(TPyP)\cdot(\mathbf{4})_2][Ru(CO)(TPP)]_6$. The long reaction time reflects the size of the two reactive components when compared to the total area the two reactive groups exhibit. Based on literature values for Sn–O [21] and Ru–py bond lengths[20], molecular modelling (MM2) suggests that the dimensions of the box (excluding carbonyl and *meso*-phenyl groups) are approximately 2 nm × 2 nm × 2 nm.

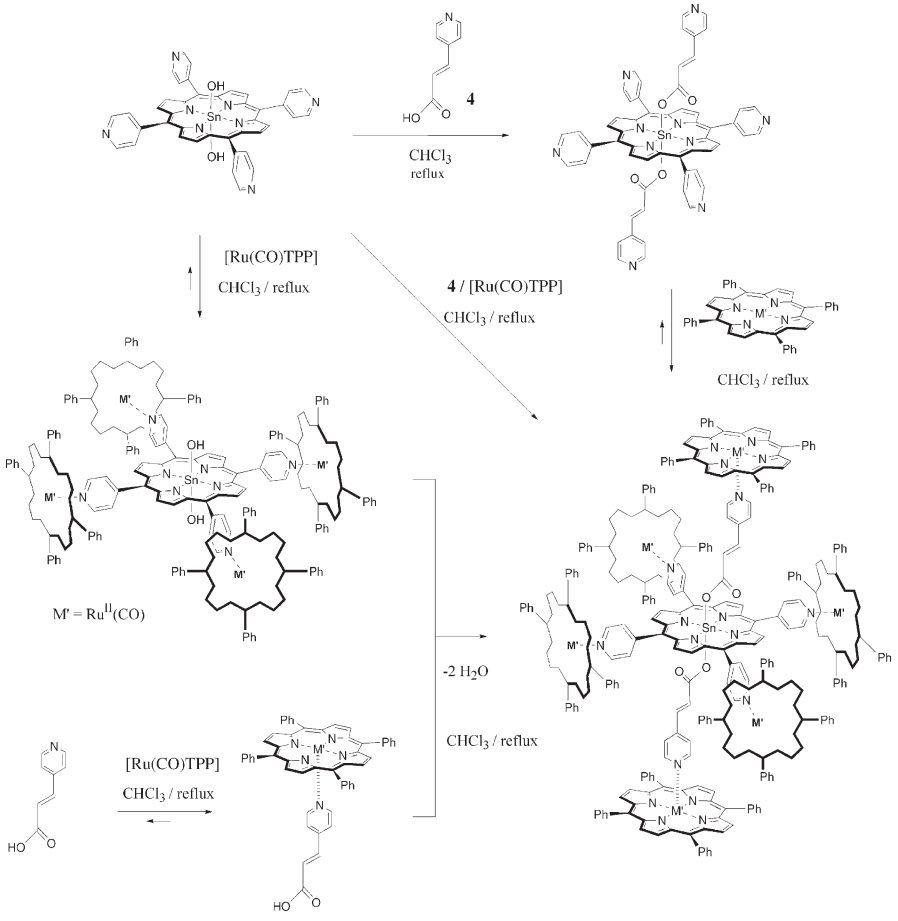

SCHEME 2

The formation of the heptameric porphyrin cube $[Sn^{IV}(TPyP)\cdot(\mathbf{4})_2][Ru(CO)(TPP)]_6$ can be achieved via three routes

Despite the close proximity of the porphyrin rings in $[Sn^{IV}(TPyP)\cdot(\mathbf{4})_2]$-$[Ru(CO)(TPP)]_6$, absorption spectra of the heptamer obtained in 10 μM $CDCl_3$ solution over the range 300–700 nm (Fig. 4) are the sum of the individual components indicating little or no molecular interaction between the porphyrin units in the ground state, consistent with the results obtained on trimeric porphyrin species[10,11].

Heteronuclear multiple quantum correlation spectroscopy (HMQC) and NOESY measurements enabled us to assign the individual proton types within the three different porphyrin environments and to ascertain through space interactions specific to the heptamer. Diagnostic peaks at δ 8.64, 8.41 and 6.77 corresponding to the β-pyrrolic protons on Ru_{eq}, Ru_{ax} and Sn porphyrins, respectively (Fig. 5), allowed for easier interpretation of the NOESY spectrum. Clearly evident within the NOESY spectrum were cross-peaks between the signals attributed to the β-pyrrolic hydrogens of the two magnetically non-equivalent sets of Ru porphyrins, indicating a close spatial orientation between them. They support the structure of the heptamer $[Sn^{IV}(TPyP)\cdot(\mathbf{4})_2][Ru(CO)(TPP)]_6$ in $CDCl_3$ (Fig. 6). The proposed structure is also supported by a set of cross-peaks resulting from the close spatial arrangement of the *meso*-aryl protons on both Ru(II) porphyrin components. All other cross-peaks generated through the NOESY experiments are intra-component, for example, showing a correlation between β-pyrrolic protons and *ortho meso*-pyridyl protons within the same porphyrin.

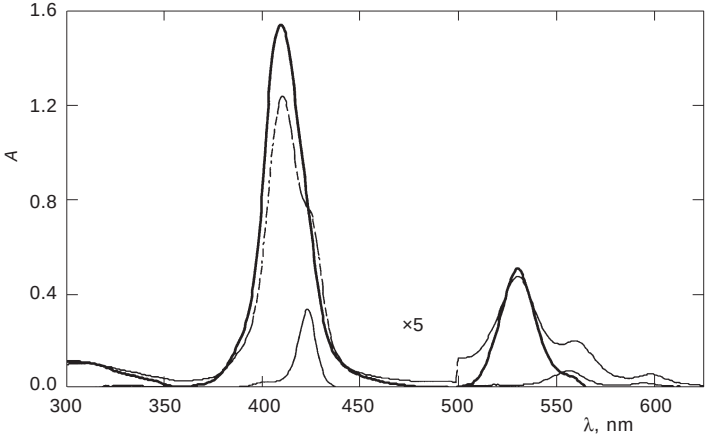

FIG. 4
UV-VIS spectra of 2 μM $[Sn^{IV}(TPyP)\cdot(\mathbf{4})_2]$ (——), $[Sn^{IV}(OH)_2(TPyP)][Ru(CO)(TPP)]_4$ (– · – ·) and $[Sn^{IV}(TPyP)\cdot(\mathbf{4})_2][Ru(CO)(TPP)]_6$ (——) in $CHCl_3$, T = 300 K

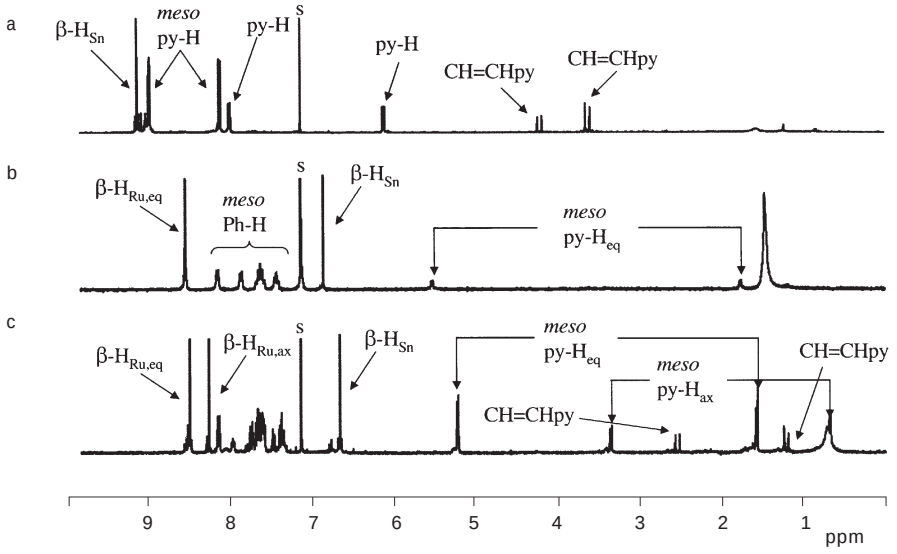

FIG. 5

^{1}H NMR spectra in $CDCl_3$ (s = residual solvent) a for [Sn^{IV}(TPyP)·(**4**)$_2$], b for [$Sn^{IV}(OH)_2$-(TPyP)][Ru(CO)(TPP)]$_4$, c for heptamer [Sn^{IV}(TPyP)·(**4**)$_2$][Ru(CO)(TPP)]$_6$

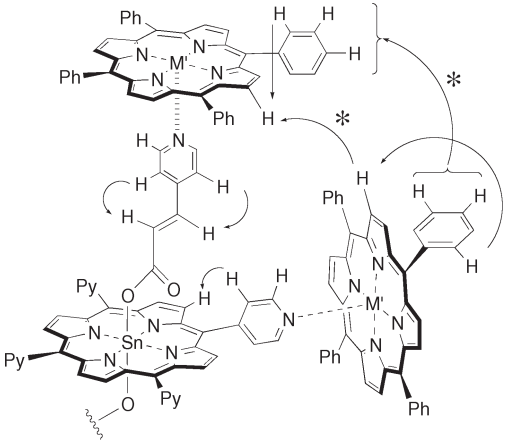

FIG. 6

Schematic representation of NOESY results obtained on the heptamer [Sn^{IV}(TPyP)·(**4**)$_2$]-[Ru(CO)(TPP)]$_6$ (500 MHz, $CDCl_3$, 293 K); the asterisk marks the results obtained by observing cross-peaks between the two different Ru(II) porphyrin types

A Multicomponent Self-Assembly Strategy in One-Pot Method

The efficiency and ease of formation of $[Sn^{IV}(TPyP)\cdot(\mathbf{4})_2][Ru(CO)(TPP)]_6$ by this stepwise approach prompted us to explore the viability of a seven-component self-assembly process around the octahedral template $[Sn^{IV}(TPyP)\cdot(\mathbf{4})_2]$ (Scheme 2). The mixing of six equivalents of [Ru(CO)-(TPP)] with $[Sn^{IV}(TPyP)\cdot(\mathbf{4})_2]$ ($CHCl_3$, reflux, 2 days) yields a very clean spectrum identical to that displayed by the final product, using the stepwise method in terms of new signals. The formation of the heptamer by this one-pot method was cleaner and more time efficient. This is readily explained by taking into account the relative reactive surface areas of the two approaches. The tecton $[Sn^{IV}(TPyP)\cdot(\mathbf{4})_2]$ with its externally radiating ligands offers an easier opportunity for reaction than the "lock-and-key" situation between $[Sn^{IV}(OH)_2(TPyP)][Ru(CO)(TPP)]_4$ and $[Ru(CO)(TPP)\cdot(\mathbf{4})]$. The ease of this self-assembly prompted us to further enhance its complexity (Scheme 2). Since each component is "pre-programmed", with respect to the level of molecular instruction it contains, to interact specifically with the other components offered within the reaction mixture, we undertook a nine-component one-pot procedure involving $[Sn^{IV}(OH)_2(TPyP)]$ (1 equivalent), [Ru(CO)(TPP)] (6 equivalents) and (**4**) (2 equivalents) in the presence of K_2CO_3 (2 equivalents). In refluxing chloroform solution, the reaction is highly efficient, forming the heptamer $[Sn^{IV}(TPyP)\cdot(\mathbf{4})_2][Ru(CO)(TPP)]_6$ as the major isolable product.

In summary, we have found that highly complex porphyrin arrays can be expediently assembled in high yields, using the non-competitive interactions of Ru(II) and Sn(IV) porphyrins. This methodology was best shown by the one-pot nine-component self-assembly of the mixed metal heptameric porphyrin box $[Sn^{IV}(TPyP)\cdot(\mathbf{4})_2][Ru(CO)(TPP)]_6$. A range of novel *pseudo*-octahedral tectons $[Sn^{IV}(TPyP)\cdot(\mathbf{1}–\mathbf{4})_2]$ that differ in the length of the axis orthogonal to the porphyrin plane have also been prepared. In the case of $[Sn^{IV}(TPyP)\cdot(\mathbf{4})_2]$, we have demonstrated that such a component will be viable for use in as templates for restrictive nano-cubes based on porphyrins. This is the goal we are currently working towards.

This research was funded through an Australian Research Council (ARC) Discovery Grant (DP0210193). Assistance with obtaining NOESY, HMQC and HSBC spectra by Dr R. Mulder at CSIRO Division of Molecular Sciences is also acknowledged.

REFERENCES AND NOTES

1. Mongin O., Schuwey A., Vollot M.-A., Gossauer A.: *Tetrahedron Lett.* **1999**, *40*, 8347.
2. Anderson H. L., Sanders J. K. M.: *Angew. Chem., Int. Ed. Engl.* **1990**, *29*, 1400.
3. Li J., Ambrose A., Yang S. I., Dier J. R., Seth J., Wack C. R., Bocian D. F., Holten D., Lindsey J. S.: *J. Am. Chem. Soc.* **1999**, *121*, 8927.
4. Elemans J. A. A. W., Nolte R. J. M., Rowan A. E.: *J. Porphyrins Phthalocyanines* **2003**, *7*, 249.
5. Takahashi R., Kobuke Y.: *J. Am. Chem. Soc.* **2003**, *125*, 2372.
6. Alessio E., Macchi M., Heath S., Marzilli L. G.: *Chem. Commun.* **1996**, 1411.
7. Slone R. V., Hupp J. T.: *Inorg. Chem.* **1997**, *36*, 5422.
8. Fan J., Whiteford J. A., Olunyuk B., Levin M. D., Stang P. J., Fliescher E. B.: *J. Am. Chem. Soc.* **1999**, *121*, 2741.
9. Drain C. M., Lehn J.-M.: *J. Chem. Soc., Chem. Commun.* **1994**, 2312.
10. Maiya B. G., Bampos N., Kumar A. A., Feeder N., Sanders J. K. M.: *New J. Chem.* **2001**, *25*, 797.
11. Fallon G. D., Langford S. J., Lee M. A. P., Lygris E.: *Inorg. Chem. Commun.* **2002**, *5*, 715.
12. Haycock R. A., Hunter C. A., James D. A., Michelsen U., Sutton L. R.: *Org. Lett.* **2000**, *2*, 2435.
13. For a recent example of other cube-like geometries, see: a) Tsuda A., Hu H., Watanabe R., Aida T.: *J. Porphyrins Phthalocyanines* **2003**, *7*, 388; b) Tsuda A., Nakamura T., Sakamoto S., Yamaguchi K., Osuka A.: *Angew. Chem., Int. Ed.* **2002**, *41*, 2817.
14. Herein, we describe a proof-of-concept to orientating the six porphyrin faces of a cube. This example uses Ru(II) porphyrins which, despite their structural stability when compared to the more labile Zn(II) porphyrins, offer an electronic disadvantage for use in light harvesting arrays, since the Ru centre quenches singlet excitation energy. This may be overcome by using Zn(II) porphyrins for template direction in preparing restrictive cubes.
15. Jasat A., Sherman J. C.: *Chem. Rev.* **1999**, *99*, 931.
16. For a recent example of a porphyrin cage, see: Fujita N., Biradha K., Fujita M., Sakamoto S., Yamaguchi K.: *Angew. Chem., Int. Ed.* **2001**, *40*, 1718. Preparing a cage from a restrictive cube by our template-directed approach would require removal of the template.
17. Hawley J. C., Bampos N., Sanders J. K. M.: *Chem. Eur. J.* **2003**, *9*, 5211.
18. Crossley M. J., Thordarson P., Wu R. A.-S.: *J. Chem. Soc., Perkin Trans. 1* **2001**, 2294.
19. Hawley J. C., Bampos N., Sanders J. K. M., Abraham R. J.: *Chem. Commun.* **1998**, 661.
20. The distances were calculated using the *Accelrys* modelling package. For Ru(II) (porphyrin)–N (pyridine) distances, see: Giribabu L., Rao T. A., Maiya B. G.: *Inorg. Chem.* **1999**, *38*, 4971.
21. Fallon G. D., Lee M. A. P., Langford S. J., Nichols P. J.: *Org. Lett.* **2002**, *4*, 1895.
22. For a recent example, see: Guldi D. M., Da Ros T., Braiuca P., Prato M., Alessio E.: *J. Mater. Chem.* **2002**, *12*, 2001.